

Preparation and characterization of alkaline phosphatase, horseradish peroxidase and glucose oxidase conjugates with carboxylated carbon nano-onions

Vibol Sok, Alex Fragoso*

Nanobiotechnology & Bioanalysis Group, Departament d'Enginyeria Química, Universitat Rovira i Virgili, Avinguda Països Catalans 26, 43007 Tarragona, Spain.

E-mail: alex.fragoso@urv.cat

Abstract

Carbon nanomaterials have emerged as suitable supports for enzyme immobilization and stabilization due to their inherently large surface area, high electrical conductivity, chemical stability and mechanical strength. In this paper, carbon nano-onions (CNOs) were used as supports to immobilize alkaline phosphatase, horseradish peroxidase and glucose oxidase. CNOs were first functionalized by oxidation to generate carboxylic groups on the surface followed by the covalent linking of the using a soluble carbodiimide as coupling agent. The CNO-enzyme conjugates were characterized by TEM and Raman spectroscopy. Thermogravimetric analysis revealed a specific enzyme load of ~0.5 mg of protein per milligram of CNO. The immobilized enzymes showed enhanced storage stability without altering the optimum pH and temperatures. These properties make the prepared nanobiocatalyst of potential interest in biosensing and other biotechnological applications.

Keywords: carbon nano-onions; enzyme immobilization; alkaline phosphatase; horseradish peroxidase; glucose oxidase

1. Introduction

Enzyme immobilization allows the reuse of the protein for an extended period of time and enables easier separation of the catalyst from the product. In most cases, immobilization improves many properties of the enzymes such as performance in organic solvents, pH tolerance, heat stability or functional stability, increasing the structural rigidity of the protein which prevents dissociation-related inactivation [1]. The improvement of enzyme properties by immobilization can be carried out using non-covalent or covalent techniques [2]. Covalent immobilization have some advantages over non-covalent immobilization, including enhanced stability and minimization of the leakage of the enzyme [3]. The selection of the optimum support material can affect the immobilization process whereby properties of both the enzyme and support material will determine the properties of the supported enzyme preparation [4].

Among the several existing supports, nanomaterials have been recently reported for enzyme immobilization and stabilization giving an inherently large surface area, which leads to high enzyme loading and consequently high volumetric enzyme activity [5]. This,

combined with a high electrical conductivity, chemical stability and strong mechanical strength makes carbon nanomaterials excellent candidates for enzyme immobilization [6]. In particular, carbon nanotubes (CNTs) have been the most explored carbon nanomaterial for this application as they are readily available and can be easily functionalized. In this sense, examples of direct physical adsorption or assisted by polymers and/or surfactants, layer-by-layer deposition and covalent linking can be found in the literature [7].

Carbon nano-onions (CNOs) are a relatively unexplored form of carbon discovered by Ugarte in 1992 [8] and formed by concentric fullerene-like layers. Similarly to CNTs, CNOs are insoluble in organic and inorganic solvents and hence a number reactions have been explored to improve their solubility and biocompatibility such as cycloaddition, oxidation with mineral acids, cyclopropanation and radical addition, among others [9]. Modified CNOs have also shown low cytotoxicity and biocompatibility [10] *in vitro* and *in vivo*. Other reported applications of CNOs include biological imaging, environmental remediation, etc. [11]

We have recently shown that CNOs can enhance the sensitivity of amperometric biosensors in DNA sensing [12]. The CNO layer can be used as support to immobilize a biorecognition element and, due to their large surface area and electronic properties, the resulting sensing platform shows enhanced performance as compared to systems not containing these nanomaterials. This has prompted us to study the immobilization of enzymes on CNOs with the aim to develop catalytic biosensors, an application that to the best of our knowledge has not been reported yet. For this, we have selected alkaline phosphatase (ALP, EC 3.1.3.1), horseradish peroxidase (HRP, EC 1.11.1.7) and glucose oxidase (GOX, EC 1.1.3.4). These enzymes are widely used in different fields such as immunoassays and electrochemical biosensors, biocatalysis and food industry, etc. [13]

2. Experimental Section

2.1 Materials

All chemicals and solvents were used as received. NaOH (2 M) was purchased from Scharlau. HCl (1 M) and GOX from *Aspergillus niger* (~200 U/mg) were purchased from Fluka. Tris(hydroxymethyl) aminomethane hydrochloride (Tris HCl), ALP from bovine intestinal mucosa (10 DEA units/mg), Alkaline Phosphatase Yellow (pNPP) Liquid

Substrate System for ELISA, magnesium chloride, D-(+)-glucose, N-(3-dimethylaminopropyl)-N'-ethylcarbodiimide hydrochloride (EDC) and Phosphate Buffered Saline (0.138 M NaCl and 0.0027 M KCl) were purchased from Sigma. 96-well microtiter plates were purchased from Fisher Scientific. *o*-Dianisidine dihydrochloride was purchased from Alfa Aesar. 2,2'-Azino-bis(3-ethylbenzthiazoline-6-sulfonic acid) (ABTS) purchased from Thermo Fisher Scientific. Horseradish Peroxidase Type IV (~60 U/mg) was purchased from Biozyme Laboratories. All solutions were prepared with water purified using a Milli-Q purification system (Millipore, 18.2 M Ω ·cm).

2.2 Instrumentation

Raman spectra were recorded in a RENISHAW inVia instrument equipped with a 514 nm excitation laser at 1 mW. A glass slide was used to hold the samples, which were lyophilized before analysis. The I_D/I_G ratio was calculated by dividing the areas of D-band and G-band peaks after background subtraction. Transmission Electron Microscopy images were recorded using an FEI TecnaiTM transmission electron microscope on Cu grids. Thermogravimetric analysis (TGA) was performed on a TGA/DSC analyzer from Mettler Toledo using a heating rate of 10°C/min until 1000°C. All samples (~ 1 mg) were measured in alumina crucibles. Samples were lyophilized in a Labconco NativeZone 1 Liter Benchtop Nativeze Dry system. Absorbances were recorded on a SpectraMax 340PC Microplate Reader on 96-well microplates at room temperature.

2.3 Preparation of oxidized CNOs

Small CNOs were obtained as recently reported [14] by annealing of nanodiamonds (5 nm nominal particle size) at 1200°C for 6 hours under argon atmosphere to afford small spherical carbon nano-onion particles of 3–4 nm diameter and 5–6 graphitic shells. The prepared CNOs were oxidized with a mixture of sulfuric and nitric acid (3:1, v/v) for one hour to give CNO-ox [15].

2.4 Covalent immobilization of HRP, ALP and GOX on CNO-ox

CNO-enzyme conjugates were prepared by amidation of CNO-ox carboxylic acid groups with the amino groups of the enzymes using EDC as coupling agent (Figure 1). For this,

10 mg of CNO-ox were suspended in 10 mL of 0.1 M acetate buffer pH 5 and sonicated for 1 hour. The solution was cooled down in an ice bath for 30 minutes then 20 mg of EDC were added. The solution was stirred for 3 hours, then 20 mg of the corresponding enzyme were added into the solution and further stirred for 4 hours maintaining the solution at 4°C. The reaction mixture was centrifuged at 4000 rpm for 10 minutes and washed several times with Tris buffer pH 7. The CNO-enzyme conjugates were dried by lyophilization for 5 hours and stored at -20°C until use. Three batches of CNO-enzyme conjugates were prepared using this procedure.

Figure 1

2.5 Kinetic assays

The activity of native ALP and CNO-ALP were measured spectrophotometrically at 405 nm based on the change of solution color of *p*-nitrophenyl groups generated by the ALP-catalyzed hydrolysis of *p*-nitrophenyl phosphate (pNPP) using Alkaline Phosphatase Yellow (pNPP) Liquid Substrate System for ELISA (Sigma). The assays were carried out at pH 6-12 and at temperatures between 20°C and 70°C in 0.1 M Tris buffer containing 0.02 M MgCl₂ pH 9 using the protocol reported by Walter and Schutt [16].

The activity of native HRP and CNO-HRP were measured spectrophotometrically at 405 nm based on the change of solution color resulting from the oxidation of ABTS by HRP in the presence of hydrogen peroxide using 1-Step™ ABTS Substrate Solution (Thermo Fisher Scientific). The assays were carried out at pH 2-8 and at temperatures between 20°C and 70°C in 0.01 M Phosphate Buffered Saline pH 7 (containing 0.138 M NaCl and 0.0027M KCl) [17].

The activity of native GOX and CNO-GOX were measured spectrophotometrically at 500 nm based on the change of solution color resulting from the HRP-catalyzed oxidation of *o*-dianisidine dihydrochloride by hydrogen peroxide produced by the oxidation of glucose by oxygen-saturated GOX. The assays were carried out at pH 4-9 and at temperatures between 20°C and 70°C in 0.01 M Phosphate Buffered Saline pH 7 (containing 0.138 M NaCl and 0.0027M KCl) [18].

For the six systems, the absorbance values were measured for 10 minutes in 10 s intervals using a microplate reader. Activities were calculated from the slope of the absorbance vs. time plots taking into account the extinction coefficient of the products formed in each reaction. In all cases, the highest activity (at optimum pH or temperature) was taken as 100%. All experiments were carried out in triplicate. In experiments comparing native with immobilized enzymes, the same amount of both enzyme forms was used in the assays.

2.6 Storage stability of native and CNO-enzyme conjugates

The storage stability of native and CNO-enzyme conjugates was determined in terms of the loss of enzyme activity after incubation of buffered solutions at 37°C in the same buffers used to measure the enzyme activity (see section 2.5). After incubation for determined periods of time, the residual activity of enzymes was measured as described above. The initial activity was considered as 100%.

3. Results and Discussion

3.1 Preparation and physicochemical characterization of CNO-enzyme conjugates

The figure 1 shows the overall procedure for the immobilization of ALP, HRP and GOX on CNOs. The first step involved an oxidation reaction to generate carboxylic groups on the graphitic shell of the CNOs to obtain CNO-ox. The carboxylic groups of CNO-ox were then linked covalently with the amino groups of the enzymes by amidation in the presence of a water soluble carbodiimide (EDC), which activates the COOH group to form a labile ester group that is further displaced by nucleophilic attack of an amino group of the enzyme to afford the corresponding CNO-enzyme conjugates (CNO-ALP, CNO-HRP and CNO-GOX). Since a large excess of both EDC and enzymes is used, enzyme self-crosslinking can occur, although most of this material is removed during the purification phase by centrifugation. The CNO conjugates formed stable suspensions when dispersed in water or buffer that did not precipitate for several days.

Figure 2 shows TEM images of the precursor CNOs and CNO-HRP. This conjugate forms small aggregates of 10-20 nm size that precipitate with time. Similar behavior was observed for CNO-ALP and CNO-GOX.

Figure 2

The TGA profiles of the CNO conjugates is strongly dependent on the amount of immobilized enzyme. This allowed the determination of the degree of functionalization of CNO-ox and CNO-enzyme conjugates by TGA analysis under an inert atmosphere from 30°C until 1000°C using pristine CNOs as reference under the same conditions (Figure 3). From the TGA curves it can be seen that CNO decomposition starts at 500°C and continues decomposing until 750°C while CNO-ox exhibit two different thermal stages with a total mass loss of 3.7% between 150°C and 450°C, corresponding to the loss of the carboxylic groups from the surface of the CNOs with a further decomposition starting at 460°C.

Figure 3

According to HRTEM images (Figure 2a), the starting CNOs have an average of six graphitic shells [14]. Considering the core is a C₆₀ fullerene, the number of carbon atoms in each shell is estimated as $60 \times n^2$ where n is the shell number, so the first shell contains $60 \times 1^2 = 60$ carbon atoms, the second shell $60 \times 2^2 = 240$ carbon atoms, and so on. Thus, the total number of carbon atoms in one CNO containing 6 shells is 5460 with a molecular weight of $5460 \times 12 \text{ g/mol} = 65\,520 \text{ g/mol}$. The loss of weight of about 3.7% in CNO-ox indicates that there are ~56 COOH groups per CNO (~1 per every 38 carbons of the outer shell). This value is smaller than the result reported previously by our group [15] due to a lower oxidation time used to avoid the generation of a large number of defects on the surface of the CNOs.

The CNO-ALP, CNO-HRP and CNO-GOX conjugates exhibit two main different thermal stages below 520°C with a total mass loss of 35%, 50% and 33%, respectively, corresponding to the decomposition of the proteins immobilized on the surface of the CNOs. In these cases, the decomposition of the carbon nanostructure takes place at temperatures ~100°C lower than that of pristine CNOs. This behavior is typical for modified carbon nanostructures. It is also noteworthy that the immobilized enzymes show, in general, a higher thermal stability than their native counterparts which decompose

completely below 460°C, further confirming the covalent immobilization of the enzymes on the CNO surface and a positive effect of the conjugation on the stability of the enzymes. From the results of the TGA analysis, the enzyme/CNO ratios were calculated taking into account the mass loss below 500°C and the molecular weight of the enzymes (Table 1). For ALP and GOX (M = 160 kDa) the results indicate that there are, on average, 5 CNO particles per enzyme, while for HRP (M = 44 kDa) three enzyme molecules are covalently linked with 2 CNOs (Table 1).

The Raman spectra at 514 nm of CNO-ALP, CNO-HRP and CNO-GOX conjugates (Figure 4) show the typical D (~1340 cm⁻¹) and G (~1580 cm⁻¹) bands characteristic of the graphitic layers of the fullerene structure of CNOs. The 2D band is also visible at ~2700 cm⁻¹. In all cases, the I_D/I_G ratio remains essentially unaltered with respect to CNO-ox (~1.0), indicating that the conjugation of the enzymes does not induce further defects in the CNO structure. The presence of the enzymes in the conjugates is visible by the appearance of new broad bands around 1100 cm⁻¹ (C-N modes) and 2900 cm⁻¹ (C-H modes), while weak bands corresponding to the amide bonds appear at ~1440 cm⁻¹ overlapped in part between the D and G bands [19].

Figure 4

3.2 Enzymatic activity of native enzymes and CNO-enzyme conjugates

Table 2 reports the catalytic properties of natives and CNO-conjugated enzymes. The CNO-ALP and CNO-GOx conjugates retained 71 and 78% of the catalytic activity of the native enzyme, while CNO-HRP kept up to 60%. This reduction could be originated from some steric hindrance produced by the attachment of the enzymes to the CNO matrix which could hinder in part the access of substrate to the active site of trypsin. Other causes could be the conditions used in the coupling reaction (pH 5, long conjugation time). However, the reduction in enzymatic activity in the CNO-enzyme conjugates was compensated by the improved stability properties, as demonstrated in the following sections. Meanwhile, the catalytic efficiency (kcat/Km) was not markedly affected by the conjugation.

3.3 Effect of pH and temperature on the catalytic activity of native enzymes and CNO-enzyme conjugates

Solution pH is one of the most important factors in enzyme activity. The effect of pH on catalytic activities of native ALP and CNO-ALP is shown in Figure 5a, which shows that both CNO-ALP and native ALP reached the maximum activity at the optimum pH 9 and also the same activity at pH 8 with 95% of the maximum activity. Hence, the immobilization did not affect the optimum pH of alkaline phosphatase. For pH values lower than 8, the activities of both enzyme forms are very similar. Interestingly, CNO-ALP shows a higher activity at pH higher than the optimum pH with 12-15% of enhancement between pH 10 and 11. This behavior of immobilized ALP is similar to that reported by Hanachi et al. [20] who covalently immobilized ALP on collagen fiber using EDC as coupling agent and may be due to the presence of unmodified carboxylate groups in the surface of the CNOs that could act as a kind of a buffer system extending the pH range of activity of the enzyme.

In the case of native HRP and CNO-HRP (Figure 4b), both forms reach the maximum activities at the same value of pH 3 meaning that the immobilization did not affect the optimum pH of the enzyme. Between pH 3 and 6, the activity of the CNO-HRP conjugate remained above 85% of the maximum activity, in agreement with other reports on HRP covalently immobilized on MWCTNs [21] using 1-pyrenebutanoic acid succinimidyl ester as a coupling agent. Figure 4c shows the effect of pH on catalytic activities of native GOX and CNO-GOX. Both native GOX and CNO-GOX reach their maximum activity at pH 6 and the activity of both enzymes is essentially the same in the studied pH range. This behavior has also been found for the conjugation of GOX with other supports such as polymer membranes [22] or silica foams [23].

Figure 5

3.4 Effect of temperature on the catalytic activity of native enzymes and CNO-enzyme conjugates

Temperature is another of the most important factors in enzyme activity. The effect of the temperature on the catalytic activities of native ALP and CNO-ALP is shown in the Figure

6a. Both native ALP and CNO-ALP reach the maximum activity at the same optimum temperature of 50°C. CNO-ALP shows between 10% and 20% higher activity than native ALP in the whole interval of temperatures, indicating that CNOs have the ability to enhance the activity of ALP when they are conjugated without altering the optimum temperature. This is in contrast to the results reported by Hanachi et al. [20] who found a lower optimum temperature for ALP immobilized on collagen fibers (40°C).

In the case of CNO-HRP and CNO-GOX, the activity vs. temperature profiles are very similar to those of the native enzymes (Figure 6b,c). The optimum temperature was found at 40°C in both cases, with no alteration with respect to the native enzyme. Conjugation to the CNOs affords more stable conjugates, especially in the case of HRP, which retains more than 50% of its initial activity at 60°C. For CNO-GOX, the conjugate retained more than 70% of activity even at 70°C, indicating that it can be effectively used in a wide temperature range as compared to GOX.

Figure 6

3.5 Storage stability of CNO-enzyme conjugates

The storage stability was studied for conjugates stored in buffer solution at 37°C for a given period of time and the kinetic measurements were carried out at the optimum pH and temperature for each system at room temperature. These conditions were selected as it is common to study the storage properties of biomolecules in so called “accelerated” conditions at relatively high temperatures in the absence of stabilizers.

As shown in Figure 7a, the results of thermal stability studies of native ALP and CNO-ALP incubated in Tris buffer pH 9 indicate a slight improvement of the stability of ALP immobilized on CNOs. The native ALP lost 67% of its initial activity whereas CNO-ALP lost 40% of its initial activity after one day. After one week, the native ALP was completely inactivated while CNO-ALP retained 18% of its initial activity, which is equivalent to the activity of native ALP after being incubated for two days.

From the results of the thermal stability studies of native HRP and CNO-HRP stored PBS buffer at pH 6 and 37°C (Figure 7b), it is clearly evident that the thermal stability of the HRP immobilized on CNO was strongly improved compared to the native HRP. The native

HRP lost 95% of its initial activity after a 5-day storage while CNO-HRP retained 50% of activity. It is interesting to note that the stability profile of CNO-HRP is similar to that of HRP conjugated to an antibody [24]

In the case of GOX, this is a thermally more stable enzyme and hence its storage stability could be studied for a longer period of time. As shown in Figure 7c, the results of the thermal stability studies of native GOX and CNO-GOX stored in PBS buffer at pH 6 and 37°C indicate that GOX immobilized on CNO retained ~90% of activity even after six weeks of storage, while native GOX lost 50% of its initial activity.

In all cases, the conjugates stored in buffer at 4°C retained more than 95% of activity after several weeks of storage. On the other hand, the CNO-HRP conjugate was more resistant to denaturation in the presence of 2 M urea (21% activity loss) than native HRP (40% activity loss). The increased stability observed for the immobilized enzymes on CNOs might be attributed to a reduction in the enzyme structure mobility due to the anchorage to the support and subsequent translation of the rigidity to the enzyme structure thus shielding it from the denaturing effects of the environment.

Figure 7

4. Conclusions

ALP, HRP and GOX have been successfully immobilized on COOH-containing CNOs by amidation reactions and characterized by TEM and Raman spectroscopy. TGA analysis indicate a specific immobilization load of ~0.5 mg of protein per mg of CNOs. The conjugates retained the same optimum pH and temperature as compared with the native enzymes, with a slight improvement of their activities and are stable for longer periods of time after storage at 37°C. These properties make the prepared nanobiocatalyst of potential interest in biosensing and other biotechnological applications.

Acknowledgements

VS thanks Generalitat de Catalunya for a pre-doctoral scholarship (grant 2015FI_B00523).

References

1. a) Sheldon, R.A.; van Pelt, S. Enzyme immobilisation in biocatalysis: why, what and how. *Chem. Soc. Rev.* 2013, 42, 6223–6235. b) Guzik, U., Hupert-Kocured, K.; Wojcieszynska, D. Immobilization as a strategy for improving enzyme properties - Application to oxidoreductases. *Molecules* 2014, 19, 8995-9018.
2. Brady, D.; Jordaan, J. Advances in enzyme immobilization. *Biotechnol. Lett.* 2009, 31, 1639-1650.
3. a) Zucca, P.; Sanjust, E. Inorganic materials as supports for covalent enzyme immobilization: methods and mechanisms. *Molecules* 19 2014, 14139-14194. b) Cui, J.; Jia, S. Optimization protocols and improved strategies of cross-linked enzyme aggregates technology: current development and future challenges. *Crit. Rev. Biotechnol.* 2015, 35, 15-28.
4. Mohamad, N. R.; Marzuki, N. H.C.; Buang, N. A.; Huyop, F.; Wahab, R. A. An overview of technologies for immobilization of enzymes and surface analysis techniques for immobilized enzymes. *Biotechnol. Equip.* 2015, 29, 205-220.
5. a) Ansari, S. A.; Husain, Q. Potential applications of enzymes immobilized on/in nano materials: A review. *Biotechnol. Adv.* 2012, 30, 512-523. b) Oliveira, S. F.; Bisker, G.; Bakh, N. A.; Gibbs, S. L.; Landry, M. P.; Strano, M. S. Protein functionalized carbon nanomaterials for biomedical applications. *Carbon* 2015, 95, 767-779.
6. Zhu, Z.; Garcia-Gancedo, L.; Flewitt, A. J.; Xie, H.; Moussy, F.; Milne, W. I. A critical review of glucose biosensors based on carbon nanomaterials: carbon nanotubes and graphene. *Sensors* 2012, 12, 5996-6022.
7. Feng, W.; Ji, P. Enzymes immobilized on carbon nanotubes. *Biotechnol. Adv.* 2011, 29, 889-895.
8. Ugarte, D. Curling and closure of graphitic networks under electron beam radiation. *Nature* 1992, 359, 707-709.
9. a) Palkar, A.; Melin, F.; Cardona, C. M.; Elliott, B.; Naskar, A. K.; Edie, D. D.; Kumbhar, A.; Echegoyen, L. Reactivity differences between carbon nano onions (CNOs) prepared by different methods. *Chem. Asian J.* 2007, 2, 625-633. b)

- Rettenbacher, A. S.; Perpall, M. W.; Echegoyen, L.; Hudson, J.; Smith, D. W. Radical addition of a conjugated polymer to multilayer fullerenes (carbon nano-onions). *Chem Mater.* 2007, 19, 1411-1417. c) Molina-Ontoria, A.; Chaur, M. N.; Plonska-Brzezinska, M. E.; Echegoyen, L. Preparation and characterization of soluble carbon nano-onions by covalent functionalization employing a Na-K alloy. *Chem. Commun.* 2013, 49, 2406-2408.
10. a) Sonkar, S. K.; Gosh, M.; Roy, M.; Begun, A.; Sarkar, S. Carbon nano-onions as nontoxic and high-fluorescence bioimaging agent in food chain an in vivo study from unicellular *E. coli* to multicellular *C. elegans*. *Mater. Express.* 2012, 2, 105-114. b) Luszczyn, J.; Plonska-Brzezinska, M. E.; Palkar, A.; Dubis, A. T.; Simionescu, A.; Simioescu, D. T.; Kalska-Szostko, B.; Winkler, K.; Echegoyen, L. Small nontocytotoxic carbon nano-onions: first covalent functionalization with biomolecules. *Chem. Eur. J.* 2010, 16, 4870-4880.
 11. a) Bartelmess, J.; Giordani, S. (2014) Carbon nano-onions (multi-layer fullerenes): chemistry and applications. *Beilstein J. Nanotechnol.*, 5, 1980-1998. b) Kausar, A. Carbon nano-onion as versatile contender in polymer compositing and advance application. *Fuller. Nanotub. Car. N.* 2017, 25, 109-123.
 12. Bartolome, J. P.; Echegoyen, L.; Fragoso, A. Reactive carbon nano-onion modified glassy carbon surfaces as DNA sensors for human papillomavirus oncogene detection with enhanced sensitivity. *Anal Chem.* 2015, 87, 6744-6751.
 13. a) Pavlidis, I. V.; Vorhaben, T.; Tsoufis, T.; Rudolf, P.; Bornscheur, U. T.; Gournis, D.; Stamatis, H. Development of effective nanobiocatalytic systems through the immobilization of hydrolases on functionalized carbon-based nanomaterials. *Bioresour. Technol.* 2012, 115, 164-171. b) Krainer, F. W.; Glier, A. An updated view on horseradish peroxidases: recombinant production and biotechnological applications. *App, Microbiol. Biotechnol.* 2015, 99, 1611-1625. c) Bankar, S. B.; Bule, M.V.; Singhal, R. S.; Ananthanarayan, L. Glucose oxidase – An overview. *Biotechnol. Adv.* 2009, 27, 489-501.
 14. Bartolome, J. P.; Fragoso, A. Preparation and characterization of carbon nano-onions by nanodiamond annealing and functionalization by radio-frequency Ar/O₂ plasma. *Fuller. Nanotub. Car. N.* 2017, 25, 327-334.

15. Wajs, E.; Molina-Ontoria, A.; Nielsen, T. T.; Echegoyen, L.; Fragoso, A. Supramolecular solubilization of cyclodextrin-modified carbon nano-onions by host–guest interactions. *Langmuir* 2015, 31, 535-541.
16. Walter, K.; Schütt, C. (1974) Alkaline phosphatase in serum. In: Bergmeyer, H. U., *Methods of Enzymatic Analysis*. 2nd edn. New York, USA, Academic Press, pp. 860–864.
17. Childs, R. E.; Bardsley, W. G. The steady-state kinetics of peroxidase with 2,2'-azino-di-(3-ethyl-benzthiazoline-6-sulphonic acid) as chromogen. *Biochem. J.* 1975, 145, 93–103.
18. Li, D.; He, Q.; Cui, Y.; Duan, L.; Li, J. Immobilization of glucose oxidase onto gold nanoparticles with enhanced thermostability. *Biochem. Biophys. Res. Commun.* 2007, 355, 488-493.
19. Rygula, A.; Majzner, K.; Marcek, K. M.; Kaczor, A.; Pilarczyk, M.; Baranska, M. Raman spectroscopy of proteins: a review. *J. Raman Spectrosc.* 2013, 44, 1061-1076.
20. Hanachi, P.; Jafary, F.; Jafary, F.; Motamedi, S. Immobilization of alkaline phosphatase on collagen surface via cross-linking method. *Iran. J. Biotech.* 2015, 13, 32-38.
21. Kim, B. J.; Kang, B. K.; Bahk, Y. Y.; Yoo, K. H.; Lim, K. J. Immobilization of horseradish peroxidase on multi-walled carbon nanotubes and its enzymatic stability. *Curr. Appl. Phys.* 2009, 9, e263-e265.
22. Rauf, S.; Ihsan, A.; Akhtar, K.; Ghauri, M. A.; Rahman, M.; Anwar, M. A.; Khalid, M. A. Glucose oxidase immobilization on a novel cellulose acetate-polymethylmethacrylate membrane. *J. Biotechnol.* 2006, 121, 351-360.
23. Balistreri, N.; Gaboriau, D.; Jolival, C.; Launay, F. Covalent immobilization of glucose oxidase on mesocellular silica foams: Characterization and stability towards temperature and organic solvents. *J. Mol. Catal. B Enzym.* 2016, 127, 26-33.
24. Laboria, N.; Fragoso, A.; O'Sullivan, C. K. Storage properties of peroxidase labeled antibodies for the development of multiplexed packaged immunosensors for cancer markers. *Anal. Lett.* 2011, 44, 2019-2030.

Table 1. Average composition and specific enzyme load for the prepared CNO-enzyme conjugates (ENZ = ALP, HRP or GOX).

| Conjugate | Molar composition (CNO) _x (ENZ) _y | | Specific enzyme load (mg/mg CNO) |
|-----------|--|----------|-------------------------------------|
| | <i>x</i> | <i>y</i> | |
| CNO-ALP | 5 | 1 | 0.49 |
| CNO-HRP | 2 | 3 | 0.44 |
| CNO-GOX | 5 | 1 | 0.49 |

Table 2. Catalytic properties of native and CNO-enzyme conjugates.

| Enzyme form | V_{max} (nM/s) | k_{cat} (s⁻¹) | K_m (M) | k_{cat}/K_m (M⁻¹ s⁻¹) |
|--------------------|-----------------------------------|---|------------------------------|--|
| ALP | 151 ± 2 | 20.1 ± 0.2 | (2.7 ± 0.3)×10 ⁻⁵ | 7.3×10 ⁵ |
| CNO-ALP | 120 ± 2 | 13.1 ± 0.1 | (2.5 ± 0.2)×10 ⁻⁵ | 5.1×10 ⁵ |
| HRP | 87 ± 1 | 15.0 ± 0.6 | (6.9 ± 0.4)×10 ⁻⁵ | 2.2×10 ⁵ |
| CNO-HRP | 50 ± 1 | 6.4 ± 0.2 | (3.3 ± 0.2)×10 ⁻⁵ | 1.9×10 ⁵ |
| GOX | 134 ± 2 | 530 ± 5 | (4.3 ± 0.1)×10 ⁻² | 1.2×10 ⁴ |
| CNO-GOX | 96 ± 1 | 305 ± 3 | (3.6 ± 0.2)×10 ⁻² | 8.5×10 ³ |

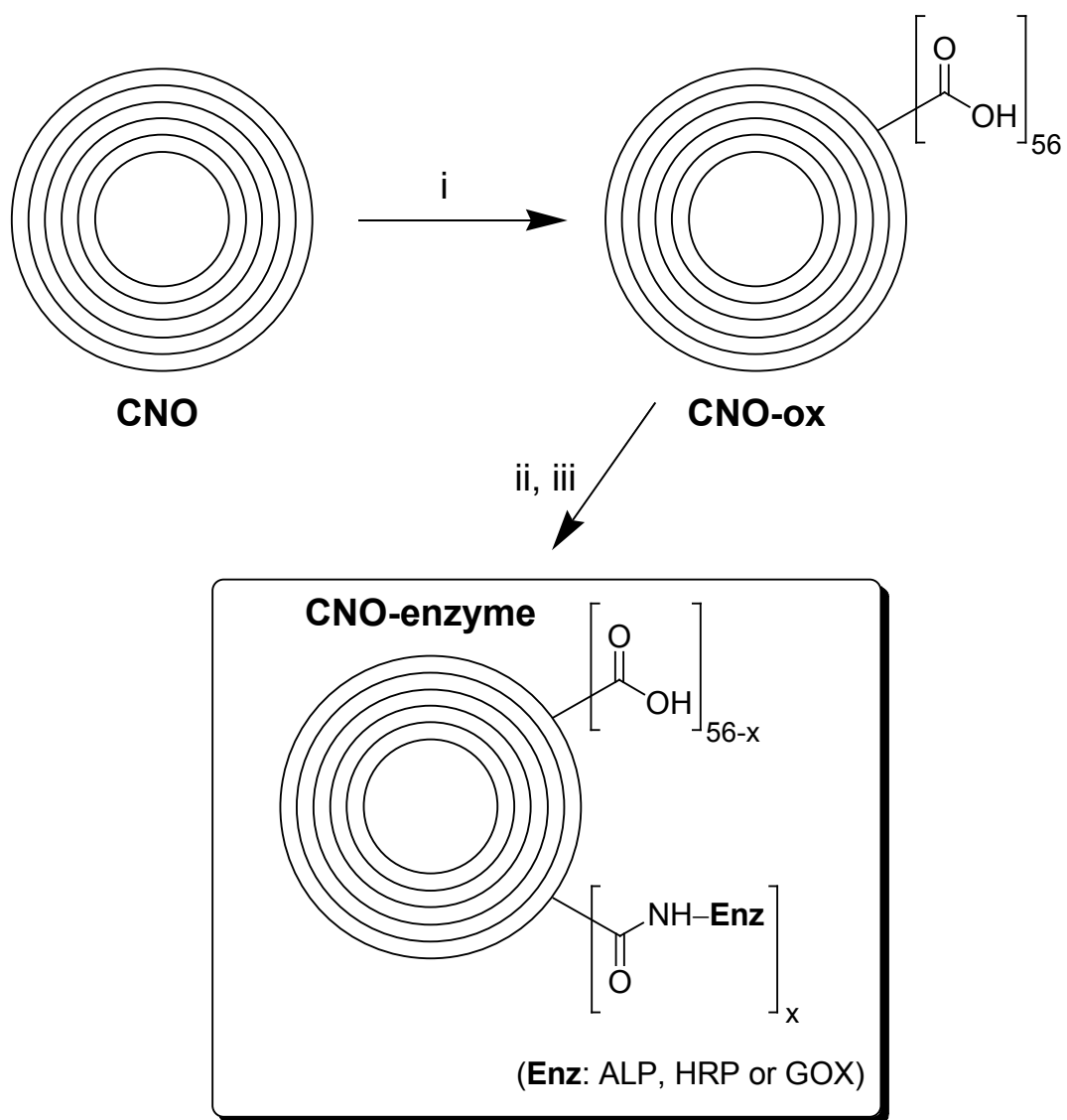


Figure 1: Preparation of CNO-enzyme conjugates. i) $\text{HNO}_3/\text{H}_2\text{SO}_4$ (3:1), ii) EDC, acetate buffer pH 5, iii) ALP, HRP or GOX.

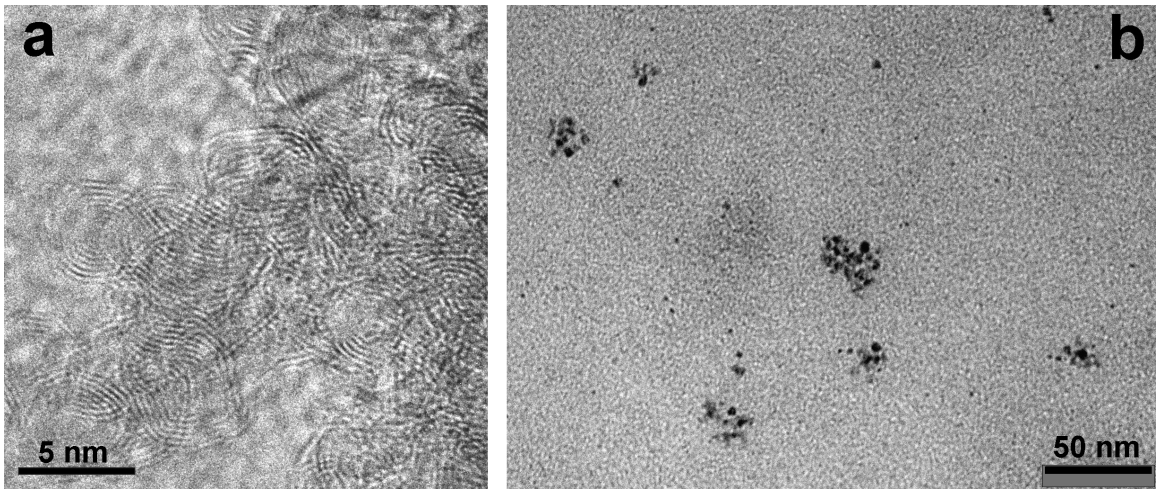


Figure 2: a) HRTEM image of the precursor CNOs. b) TEM image of CNO-HRP suspended in water.

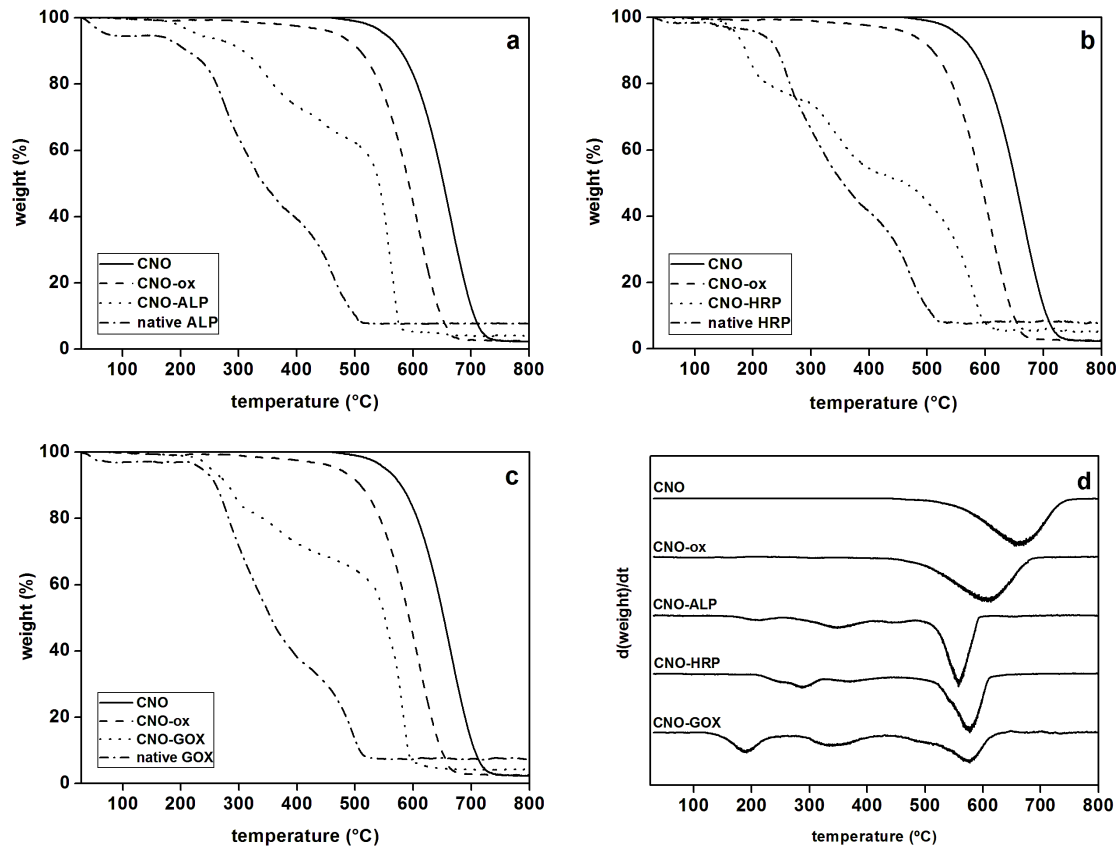


Figure 3: TGA curves of CNOs, CNO-ox and CNO-enzyme conjugates (a-c) and first derivative curves (d).

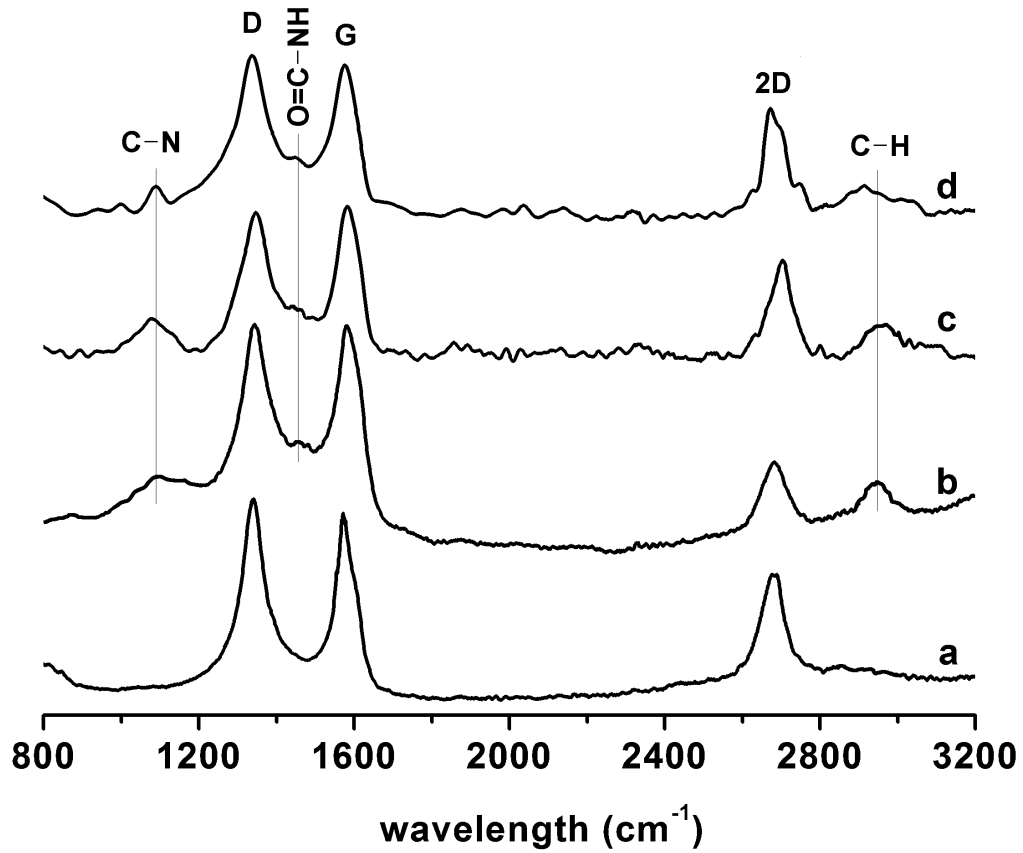


Figure 4: Raman spectra (514 nm) CNO-ox (a), CNO-ALP (b), CNO-HRP (c) and CNO-GOX (d).

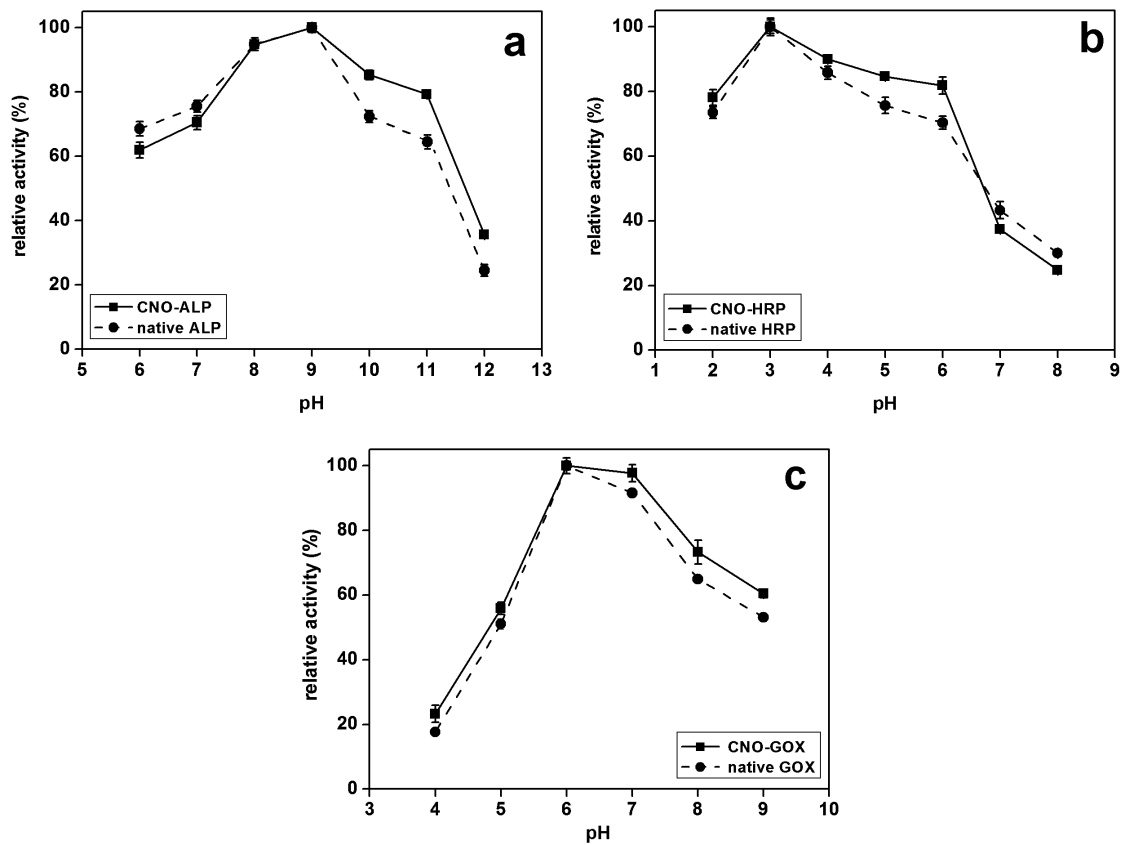


Figure 5. Activity vs. pH profile for native and CNO-conjugated enzymes.

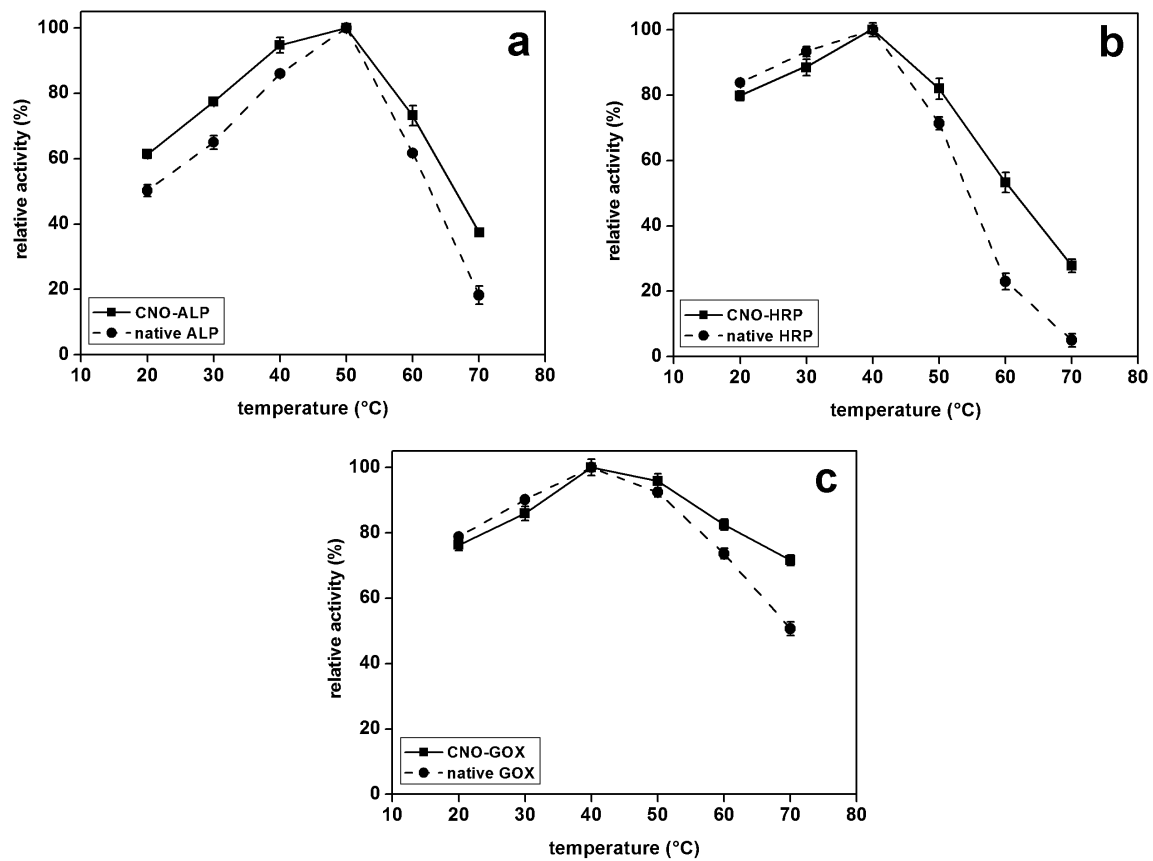


Figure 6. Activity vs. temperature profile for native and CNO-conjugated enzymes.

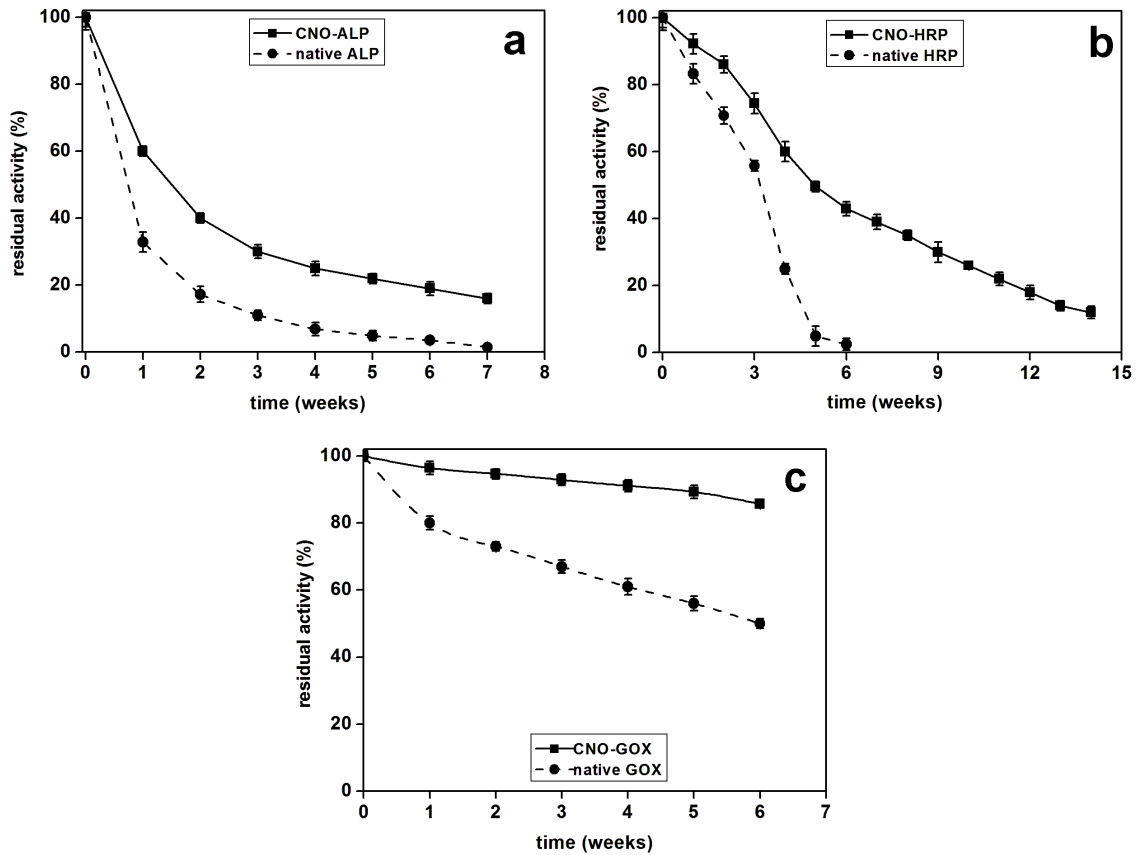


Figure 7. Residual enzymatic activity of native and CNO-conjugated enzymes stored in buffer solution at 37°C (see text for details).